

---

## Research Paper

---

# Molecular Mobility in Raffinose in the Crystalline Pentahydrate Form and in the Amorphous Anhydrous Form

Joaquim J. Moura Ramos,<sup>1</sup> Susana S. Pinto,<sup>2</sup> and Hermínio P. Diogo<sup>2,3</sup>

Received February 1, 2005; accepted April 25, 2005

**Purpose.** The aims of the study are to characterize the slow molecular mobility in solid raffinose in the crystalline pentahydrate form, as well as in the anhydrous amorphous form ( $T_g = 109^\circ\text{C}$  at  $5^\circ\text{C}/\text{min}$ ), and to analyze the differences and the similarities of the molecular motions in both forms.

**Methods.** Thermally stimulated depolarization current (TSDC) is used to isolate the individual modes of motion present in raffinose, in the temperature range between  $-165$  and  $+60^\circ\text{C}$ . From the experimental output of the TSDC experiments, the kinetic parameters associated with the different relaxational modes of motion were obtained, which allowed a detailed characterization of the distribution of relaxation times of the complex relaxations observed in raffinose. The features of the glass transition relaxation in raffinose were characterized by differential scanning calorimetry (DSC).

**Results.** A complex mobility was found in the crystalline form of raffinose. From the analysis of the TSDC data, we conclude that these molecular motions are local and noncooperative. A sub- $T_g$  relaxation, or secondary process, was also detected and analyzed by TSDC in the amorphous phase. It has low activation energy and low degree of cooperativity. The glass transition was studied by DSC. The fragility index (Angell's scale) of raffinose obtained from DSC data is  $m = 148$ .

**Conclusions.** TSDC proved to be an adequate technique to study the molecular mobility in the crystalline pentahydrate form of raffinose. In the amorphous form, on the other hand, the secondary relaxation was analyzed by TSDC, but the study of the glass transition relaxation was not possible by this experimental technique as a consequence of conductivity problems. The DSC study of the glass transition indicates that raffinose is an extremely fragile glass former.

**KEY WORDS:** fragility; glass transition; secondary relaxations; thermally stimulated currents; TSDC.

## INTRODUCTION

Raffinose, also known as melitose, is a nonreducing trisaccharide containing galactose and sucrose and is frequently found in plants. It is well known that some sugars such as lactose, raffinose, and trehalose could act as cryo- and lyoprotectants of proteins, liposomes, and related pharmaceutical materials and are found in desiccation-resistant organisms (1,2). A nonreducing sugar is a request for protein stabilization due to their capacity to form amorphous freeze-concentrates avoiding Millard reactions. In addition, these sugars when used as solutes are required to form a single amorphous phase with the protein without phase separation. The mechanism by which these sugars help to protect the integrity of such materials is not completely understood, but this ability seems to be a consequence of two factors: specific hydrogen-bonding interactions between the sugar and the protein outer surface which helps to maintain the three-

dimensional structure of the protein, and of their tendency to provide a viscous glassy state, allowing to a nonspecific restriction of conformational flexibility of the protein (3). In this context, the study of the evolution of the molecular mobility from high temperature down to the glassy state is a relevant aspect to the understanding of the biopreservation ability. Despite the frequent use of sugars as protecting agents, little is known about molecular mobility in glassy sugars. The molecular mobility of amorphous pharmaceutical materials, which incorporate sugars in the formulation, is known to be a key factor in determining their physicochemical properties, stability, and reactivity. Usually, such molecular mobility is quantified using relaxation time constants. Furthermore, the whole pattern of the mobility changes in glass-forming systems, as a function of temperature, is actually the object of an active fundamental research in physics. The impact of the molecular mobility features in biopreservation thus appears as a problem that deserves a special attention.

The structural features of the crystalline forms of raffinose as well as the characterization of the glass transition relaxation were reported in previous works (4,5). The reported activation enthalpy of structural relaxation (5) was obtained by integrating the differential scanning calorimetry (DSC) relaxation endothermic (overshoot in the heat flow)

<sup>1</sup> Centro de Química-Física Molecular, Complexo I, IST, Av. Rovisco Pais, 1049-001 Lisbon, Portugal.

<sup>2</sup> Centro de Química Estrutural, Complexo I, IST, Av. Rovisco Pais, 1049-001 Lisbon, Portugal.

<sup>3</sup> To whom correspondence should be addressed. (e-mail: hdiogo@ist.utl.pt)

for different sub- $T_g$  annealing times. In the present work, we obtain the same dynamic parameter using a different procedure, based on the heating rate dependence of the onset temperature of the DSC glass transition signal. The dielectric experimental technique of thermally stimulated depolarization current (TSDC) will also be used to study the slow molecular mobility in solid raffinose, in the crystalline pentahydrate form, as well as in the anhydrous glassy form.

## MATERIALS AND METHODS

D(+)-Raffinose pentahydrate ( $C_{18}H_{32}O_{16} \cdot 5H_2O$ , CAS no. 17629-30-0) was purchased from Acros, Somerville, NJ, USA (catalogue no. 19567, 99+% purity) and was used without further purification. The chemical structure of this substance is shown in Fig. 1.

Amorphous raffinose was prepared by freeze-drying a 0.056 M aqueous solution of raffinose using a Lyoalfa commercial apparatus, model 6-80, provided by Telstar Industrial, Barcelona, Spain. The raffinose solution was first frozen in liquid nitrogen, and the primary drying was carried out during 20 h at  $-(82 \pm 5)^\circ\text{C}$  under a vacuum of  $10^{-2}$  mbar. The sample was subsequently dried in an oven at  $\approx 100^\circ\text{C}$  for 1 day to remove residual water and, finally, kept at room temperature inside a desiccator during several days before pelletization for TSDC measurements. X-ray powder diffraction was used to confirm that the freeze-dried samples were amorphous. Glassy raffinose was also prepared by cooling from the metastable liquid at  $140^\circ\text{C}$  under inert atmosphere and by complete dehydration of the crystal at  $90^\circ\text{C}$  under vacuum. We have convincing evidence that the so-called amorphous samples are not semicrystalline as checked by X-ray powder diffractometry and  $\Delta C_p$  measurements. On the other hand, we believe that no residual water is present in the amorphous samples. This belief is based on the results obtained by Karl Fischer titrimetry and on the fact that the  $T_g$  value of the samples (obtained by DSC) corresponds to that of the nonplasticized raffinose as reported by Saleki-Gerhardt et al. (6).

The DSC measurements were performed with a 2920 MDSC system from TA Instruments Inc., Newcastle, DE, USA. The samples of  $\sim 8$ – $15$  mg were introduced in aluminum pans, hermetically sealed using a sample encapsulating press. The measuring cell was continually purged with high purity helium gas at 30 mL/min. An empty aluminum pan, identical to that used for the sample, was used as reference. The baseline was calibrated scanning the temperature domain of the experiments with an empty pan. The temperature calibration was performed taking the onset of the endothermic melting peak of several calibration standards. The temperature calibration for the different heating

rates was performed considering the heating rate dependence of the onset temperature of the melting peak of indium and benzoic acid, as explained elsewhere (7). The enthalpy scale was also calibrated using indium (enthalpy of fusion:  $\Delta_{\text{fus}}H = 28.71 \text{ J g}^{-1}$ ).

Thermally stimulated depolarization current (TSDC) experiments were carried out with a TSC/RMA spectrometer (TherMold, Stamford, CT, USA) covering the range from  $-170$  to  $+400^\circ\text{C}$ . For TSDC measurements, the sample (approximately 50 mg) was placed between the electrodes of a parallel plane capacitor with effective area of  $\sim 38 \text{ mm}^2$  (thickness of  $\sim 0.5 \text{ mm}$ ). The sample is immersed in an atmosphere of high purity helium (1.1 bar). The fact that the relaxation time of the motional processes is temperature dependent and becomes longer as temperature decreases enables to immobilize them by cooling. This is the basis of the TSDC technique, which is particularly adequate to probe slow molecular motions. To analyze specific regions of the TSDC spectrum, different methods of polarizing the sample can be used, namely, the so-called TSDC global polarization experiment and the partial polarization (PP) experiment (often called thermal sampling or windowing or cleaning). The PP method, where the polarizing field is applied in a narrow temperature interval, enables to resolve a global peak into its individual relaxation modes (8). The thermal sampling procedure allows to retain (or to freeze) a polarization that arises from a narrow variety of dipolar motions. In the limit of a very narrow polarization window, the retained polarization (and, of course, the current peak that is the result of a partial polarization experiment) would correspond to a single, individual dipolar motion (9,10).

The experimental output of a TSDC experiment is the depolarization current intensity as a function of temperature, as schematically depicted in Fig. 2.

An important feature of the TSDC technique is that it allows the calculation of the temperature-dependent relaxation time,  $\tau(T)$ , of a single relaxation process from the experimental result of the corresponding PP experiment. As explained in a previous work published in this journal (10),  $\tau(T)$  is calculated from:

$$\tau(T) = \frac{\frac{1}{r} \int_T^{T_f} J(T') dT'}{J(T)} = \frac{\frac{1}{r} \int_T^{T_f} I(T') dT'}{I(T)} \quad (1)$$

where  $I(T)$  is the depolarization current intensity measured in the heating ramp of the PP experiment and  $T_f$  is a temperature well above the temperature of the maximum of the PP peak, where the sample is already completely depolarized (see Fig. 2).

The capability of directly calculating the relaxation time from the results of a single partial polarization experiment constitutes an essential quantitative feature of the TSDC technique, and that is why TSDC is an experimental technique that provides important information on molecular mobility in solids, i.e., on the kinetics of relaxational processes and on the distribution of relaxation times.

The physical background of the TSDC technique is presented elsewhere (11,12). Several recently published papers (9,10,13) can be helpful to explain the experimental procedures used in TSDC and the physical meaning of the data provided by this technique.

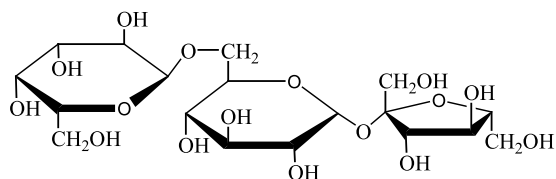


**Fig. 1.** Chemical structure of raffinose. The trisaccharide is the sequence, from left to right, of the monosaccharide moieties galactose, glucose, and fructose.

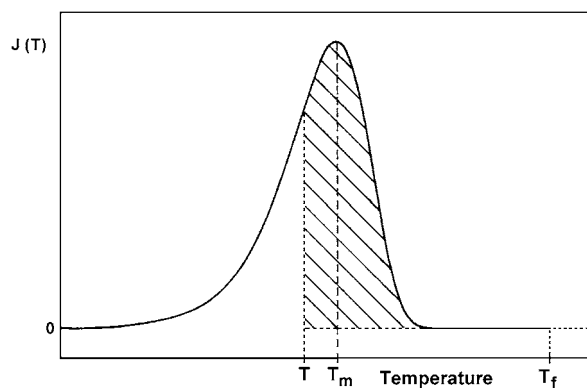


**Fig. 2.** Thermally stimulated depolarization current (TSDC) peak obtained from a partial polarization experiment. The dashed area corresponds to the integral  $\int_T^{T_m} J(T')dT'$  in Eq. (1).

## RESULTS AND DISCUSSION

The as-received sample is in the crystalline pentahydrate form. It is reported that the dehydration of the pentahydrate occurs by heating (up to a temperature of 80°C or higher) and that dehydration automatically leads to vitrification (4,5). This behavior was confirmed on our samples by DSC, and we found that the amorphous material has a calorimetric glass transition temperature at  $T_g = 109^\circ\text{C}$  (at 5°C/min), in good agreement with the previously reported value  $T_g = 103^\circ\text{C}$  obtained by DSC at 5°C/min (5) and with the value  $T_g = 106^\circ\text{C}$  obtained from the temperature dependence of the OH stretching frequency (14). It is to be noted that the endothermic peak observed by DSC at  $\sim 80^\circ\text{C}$ , which corresponds to the dehydration process, has been erroneously attributed to melting (4,6,15).

From the TSDC experiments, it was observed that a strong increase of the spontaneous current occurs above  $\sim 100\text{--}105^\circ\text{C}$ , independent of the strength (or of the presence) of the electric field. This occurrence prevents the study of the glass transition relaxation of raffinose by the TSDC technique. As a consequence, the characterization of the glass transition of raffinose was only performed on the basis of DSC results. In the following, we will also report the results of the TSDC study of the molecular mobility of solid raffinose, crystalline and amorphous. It is to be stressed that these are pure phases. In fact, the DSC thermogram of the amorphous samples did not reveal any trace of endothermic signal corresponding to dehydration, and X-ray results confirmed that no crystalline fraction was present in the amorphous samples. Moreover, no amorphous fraction was detected by DSC in the crystalline pentahydrate samples.

### General Characterization of the Molecular Mobility in Raffinose

The crystalline pentahydrate was studied by TSDC in the temperature range between  $-165$  and  $70^\circ\text{C}$  (recall that dehydration takes place at  $\sim 80^\circ\text{C}$ ). The amorphous anhydrous form was studied in the temperature range between  $-165$  and  $100^\circ\text{C}$ . The low-temperature TSDC thermogram of raffinose in the crystalline pentahydrate form (Fig. 3, thick line) shows a clear structuration of the relaxation peaks,

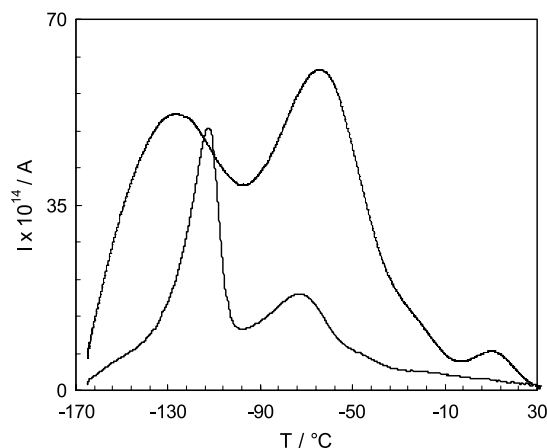
revealing a relatively strong hierarchy of the molecular motions. In fact, it shows a sharp relaxation with maximum intensity at  $-113^\circ\text{C}$ , and a lower intensity one at  $-72^\circ\text{C}$ , immersed in a broad and low-intensity relaxation background. Figure 3 also shows a TSDC thermogram of raffinose in the amorphous form (thin line), obtained with an experimental protocol identical to that used for the crystalline sample. It can be observed that the dielectric strength of the relaxational processes generally increases in the amorphous compared with the crystalline form, and that the broadness of the relaxation increases, accompanied by a loss of structuration. Two intensity maxima are, however, observed at  $-127$  and at  $-65^\circ\text{C}$  in the TSDC spectrum of amorphous raffinose.

Figure 4 shows the results of a series of partial polarization experiments carried out in the crystalline pentahydrate form.

In Fig. 4A, the partial polarization peaks correspond to the global thermogram shown in Fig. 3 (thick line). In Fig. 4B, on the other hand, presented are some PP components of a higher temperature relaxation that shows a maximum intensity at  $\sim 20^\circ\text{C}$  (temperature region not included in Fig. 3).

The amorphization of the sample was carried out in three different ways: (1) it was annealed at  $90^\circ\text{C}$ , under vacuum, for 1 h; (2) it was heated up to  $140^\circ\text{C}$  (above  $T_g$ , in the metastable liquid region), under inert atmosphere; (3) it was freeze-dried according to the procedure described in Materials and Methods. The TSDC results obtained with the three kinds of glassy sample show that they have similar dynamic features. TSDC results thus do not support the idea that different amorphization procedures can generate glasses with different properties. Figure 5 shows the results of a series of partial polarization experiments carried out in a freeze-dried sample. As noted before, the studied samples are fully amorphous.

Figure 5A shows the results of a series of PP experiments that correspond to temperature range of the global



**Fig. 3.** TSDC thermogram of raffinose in the crystalline pentahydrate form (thick line) and in the amorphous lyophilized form (thin line). The experimental protocol was exactly the same for both experiments. The sample was polarized with an electric field with strength  $E = 450$  V/mm, between the polarization temperature  $T_p = -30^\circ\text{C}$  and the freezing temperature  $T_0 = -165^\circ\text{C}$ ; the heating rate of the heating ramp was  $15^\circ\text{C}/\text{min}$ , and the final temperature of the ramp was  $T_f = 60^\circ\text{C}$ . The property in the ordinate axis is the current intensity expressed in amperes,  $I(A)$ .

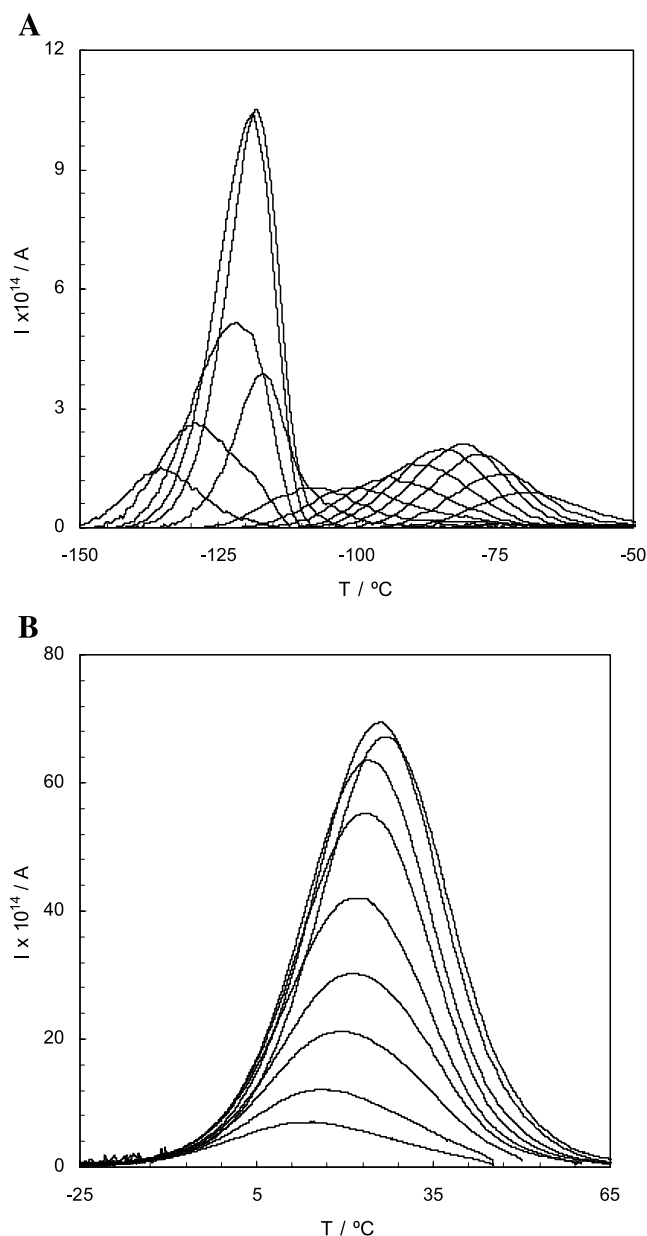


**Fig. 4.** Partial polarization components of the slow mobility of the crystalline pentahydrate raffinose obtained at a heating rate of  $4^\circ C/min$ , with a polarizing electric field of  $E = 450 V/mm$  and with a polarization window of  $\Delta T = 2^\circ C$ . The property in the ordinate axis is the current intensity expressed in ampere,  $I(A)$ . (A) Components of the low-temperature relaxation obtained with polarization temperatures from  $T_p = -140^\circ C$  up to  $T_p = -65^\circ C$ . (B) Components of the relaxation at  $\sim 20^\circ C$  obtained with polarization temperatures from  $T_p = -5^\circ C$  up to  $T_p = 20^\circ C$ .

thermogram shown in Fig. 3 (thin line). In Fig. 5B, on the other hand, presented are some PP components of a higher temperature relaxation that shows a maximum intensity at  $\sim 40^\circ C$  (temperature region not included in Fig. 3).

The activation enthalpies of the partial polarization components of the slow mobility of raffinose (some of them shown in Figs. 4 and 5) are shown in Fig. 6 as a function of the peak's location,  $T_m$ . The circles correspond to the crys-

talline pentahydrate form, whereas the triangles correspond to the anhydrous amorphous (lyophilized) form.

From Fig. 6, we can draw two main conclusions:

1. The partial polarization components of the slow mobility of solid raffinose show kinetic parameters that are similar for the crystalline pentahydrate form and for the anhydrous amorphous form (the circles and the triangles show the same evolution tendency). As suggested before, the difference in mobility between the two forms seems to be that: (a) the quantity of dipole moment (polarization or dipole

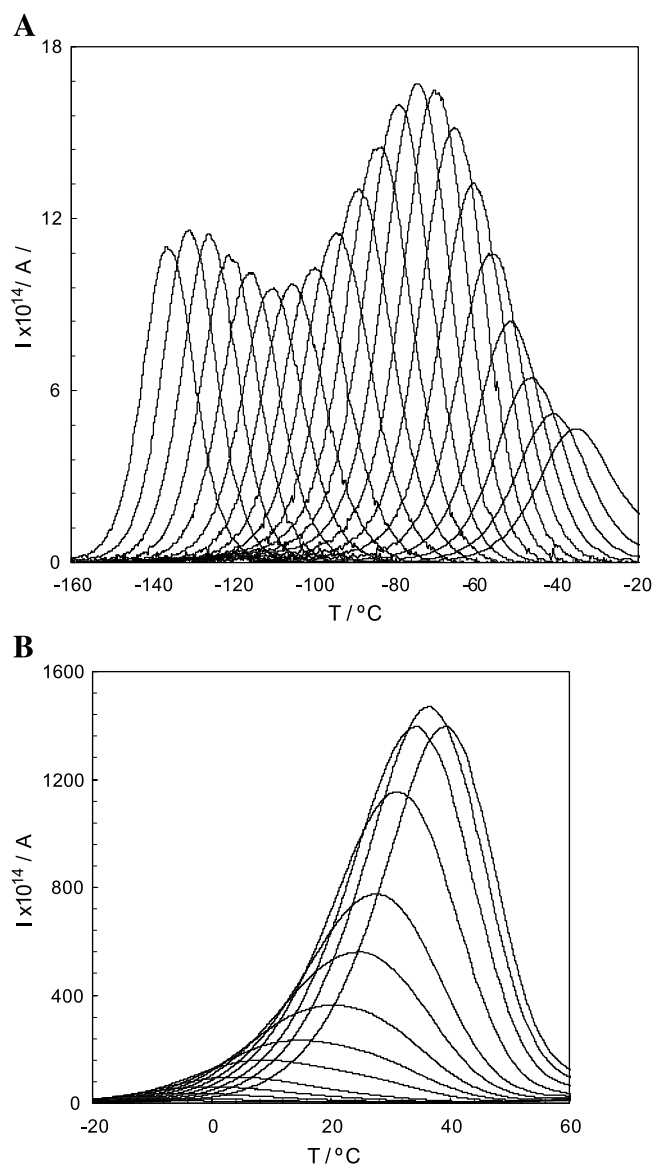


**Fig. 5.** Partial polarization components of the slow mobility of the anhydrous amorphous raffinose obtained at a heating rate of  $4^\circ C/min$ , with a polarizing electric field of  $E = 450 V/mm$ , and with a polarization window of  $\Delta T = 2^\circ C$ . The property in the ordinate axis is the current intensity expressed in ampere,  $I(A)$ . (A) Components of the low-temperature relaxation obtained with polarization temperatures from  $T_p = -140^\circ C$  up to  $T_p = -40^\circ C$ , with intervals of  $5^\circ C$ . (B) Components of the relaxation at  $\sim 40^\circ C$  obtained with polarization temperatures from  $T_p = -30^\circ C$  up to  $T_p = 35^\circ C$ , with intervals of  $5^\circ C$ .

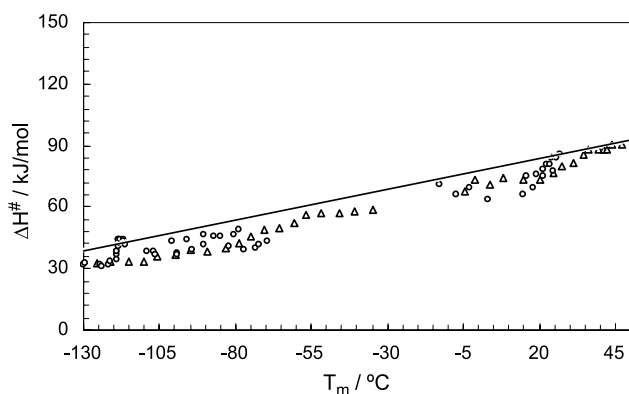


**Fig. 6.** Activation enthalpy of the partial polarization peaks of the slow mobility of raffinose, as a function of the peak's location,  $T_m$ . The uncertainty in the enthalpy values is less than 2%. The continuous line corresponds to the zero entropy prediction. The circles are relative to the crystalline pentahydrate form, whereas the triangles correspond to the anhydrous amorphous form.

moment by unit volume) involved in the relaxations is, in general, higher in the amorphous than in the crystalline pentahydrate form; and (b) the relaxations appear with a higher structuration in the crystalline form (more individualized motions), whereas they are broader in the amorphous form.

2. The individual molecular motions display a very localized nature in the crystalline as well as in the amorphous form given that the corresponding activation entropy is negligible (the points are in the proximity of the zero entropy line) (10,16).

### The Mobility in the Anhydrous Amorphous Form

In the case of the anhydrous amorphous form, the relaxations observed by TSDC, and shown in Fig. 5A and B, are sub- $T_g$  relaxations that obey to the zero entropy line (see Fig. 6). The lower temperature relaxation (Fig. 5A) displays all the features of a secondary  $\beta$ -relaxation: (1) the partial polarization components show an Arrhenius behavior and have zero activation entropy; (2) the relaxation is very broad, which arises from the fact that the corresponding molecular motions occur in a wide distribution of nearly identical environments; (3) the temperature location of the partial polarization peaks,  $T_m$ , varies linearly with the polarization temperature,  $T_p$ , with a slope near unity, as shown in Fig. 7 (triangles in the left-hand side); otherwise stated, the displacement of the peak position is nearly equal to the variation of the polarization temperature, and this is so because the shape of the partial polarization peaks (the distribution of relaxation times) does not change significantly from one value of  $T_p$  to another.

In this context, we believe that the TSDC results shown in Fig. 5A are the manifestation of the  $\beta$ -relaxation of amorphous raffinose. However, the assignment of this mobility at the molecular level is not straightforward given that the molecular origin of this relaxation is not yet fully elucidated. In general terms, it is attributed to rotational fluctuations of functional groups or to librational motions of the whole molecules. Oppositely to the lower temperature

relaxation (Fig. 5A), and despite the fact that it is also a sub- $T_g$  relaxation and that it obeys to the zero entropy line (see Fig. 6), the relaxation at  $\sim 35^\circ\text{C}$  shown in Fig. 5B does not display the basic features of a secondary  $\beta$ -relaxation. In fact, it is narrow in the temperature axis, and the representation of  $T_m$  vs.  $T_p$  (triangles in the right-hand side of Fig. 7) does not fit to the continuous line that describes the behavior of the  $\beta$ -relaxation of amorphous raffinose. The assignment of this mobility is thus a difficult task, all the more because the alternative hypothesis of a space charge phenomenon does not seem very satisfactory given that it is most often observed at temperatures above  $T_g$ , and it is often characterized by high activation entropies, i.e., strong deviations from the zero entropy line (an attribute of diffusional motions). Note, however, that the intensity of this relaxation is two orders of magnitude higher compared with that shown in Fig. 5A, which can give some credibility to the previously referred hypothesis.

### The Glass Transition of Raffinose (DSC)

As stated before, we were not allowed to study the glass transition relaxation by thermally stimulated depolarization currents, so that we tried to obtain a characterization of this relaxation using differential scanning calorimetry. Let us recall that, when heated, the crystalline pentahydrate form dehydrates causing the crystal to collapse into an amorphous form at  $\sim 80^\circ\text{C}$ . No endothermic melting peak is thus observed in the DSC scan. Furthermore, we found by DSC that no crystallization is observed on cooling from the metastable liquid, so that raffinose easily vitrifies on further cooling. The DSC signature of the glass transition is a sigmoidal change in the heat flux that arises from a change in heat capacity,  $\Delta C_p$ , when the sample is heated from the glassy state to the metastable supercooled liquid. The glass transition temperature (identified with the onset of the DSC glass transition signal) was found to be  $T_g = 109^\circ\text{C}$  (at  $5^\circ\text{C}/\text{min}$  on heating). On the other hand, the

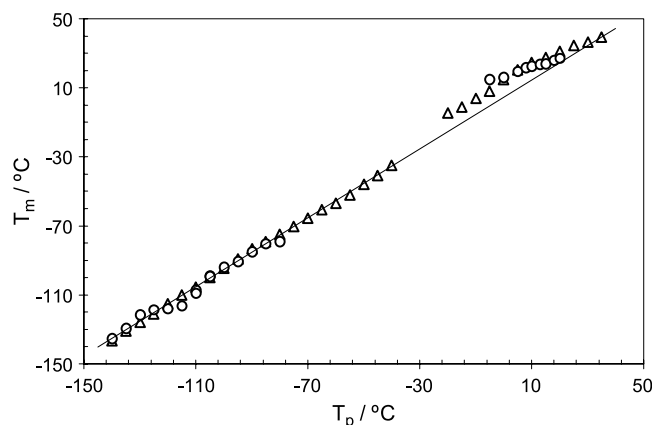


**Fig. 7.** Temperature of maximum intensity of the partial polarization peaks,  $T_m$ , as a function of the corresponding polarization temperature,  $T_p$ . The circles are relative to experiments in the pentahydrate crystalline form, whereas the triangles correspond to the anhydrous amorphous form. The continuous line was obtained by fitting the points relative to the  $\beta$ -relaxation of raffinose (triangles in the left-hand side, with  $T_p < -40^\circ\text{C}$ ).

heat capacity jump at the glass transition was found to be  $\Delta C_P = 0.55 \pm 0.01 \text{ J K}^{-1} \text{ g}^{-1} = 278 \pm 5 \text{ J K}^{-1} \text{ mol}^{-1}$  (average over 34 determinations), where the uncertainty indicated corresponds to the standard deviation of the mean.

It is well known that the temperature of the onset of the glass transition signal tends to higher temperatures as the heating (or cooling) rate increases. One of the methods of thermal analysis allowing the determination of glass-former fragility is precisely based on the scanning rate dependency of  $T_g$  (17). We thus used the DSC technique to estimate the activation enthalpy of structural relaxation at  $T_g$ ,  $E_a(T_g)$ , and the fragility index,  $m$ , of raffinose. It was shown (18) that the dependence of the glass transition temperature,  $T_g$ , on the heating or cooling rate,  $|q|$ , of a conventional DSC experiment is given by

$$\frac{d \ln |q|}{d 1/T_g} = -\frac{E_a}{R} \quad (2)$$

where  $E_a$  is the activation energy for the relaxation times controlling the structural enthalpy relaxation. The results of our experiments on the influence of the heating rate on the onset temperature,  $T_{g,\text{on}}$ , of the glass transition signal are shown in Fig. 8 where the representation of  $\ln |q|$  as a function of  $1/T$  is presented.

From the linear regression analysis of the data (points in Fig. 8), we obtain an activation energy of  $1,080 \text{ kJ mol}^{-1}$ .

The fragility index,  $m$ , of a substance was defined as the slope of the  $\log \tau(T)$  vs.  $T_g/T$  line at the glass transition temperature, i.e., at  $T = T_g$  (19,20),

$$m = \left[ \frac{d \log_{10} \tau(T)}{d(T_g/T)} \right]_{T=T_g} \quad (3)$$

where  $\tau$  is the structural relaxation time which slows down to  $\sim 100 \text{ s}$  at  $T_g$ . Eq. (3) can be expressed in terms of the apparent activation energy,  $E_a$ , as

$$m = \frac{1}{2.303} \left[ \frac{E_a(T_g)}{RT_g} \right] \quad (4)$$

The value of  $E_a$  obtained from Eq. (2) can thus be used to calculate the fragility index of a glass-forming system according to Eq. (4). Note that 16 is the limit of the Angell's scale of fragility for infinitely strong glass formers, and that glycerol and *m*-toluidine, for example, have fragilities of 49 and 85, respectively (21,22). The calculated fragility index of raffinose, considering for the glass transition temperature the value  $T_g = 109^\circ\text{C}$  (the onset of the glass transition signal for a heating rate of  $5^\circ\text{C}/\text{min}$ ), is  $m = 148$ , which indicates that we are in the presence of an extremely fragile glass former.

In general, there is a consistent trend toward larger heat capacity changes,  $\Delta C_P$ , at  $T_g$  as the liquid behavior tends to increased fragility (20). Raffinose displays behavior compatible with this trend. The interpretation in terms of the potential energy hypersurface of a macroscopic system is as follows. Fragile liquids show a proliferation of possible configurations (lack of rigid structure) so that they have a very high density of potential energy minima responsible for the high heat capacity jump at  $T_g$ . This is called thermody-

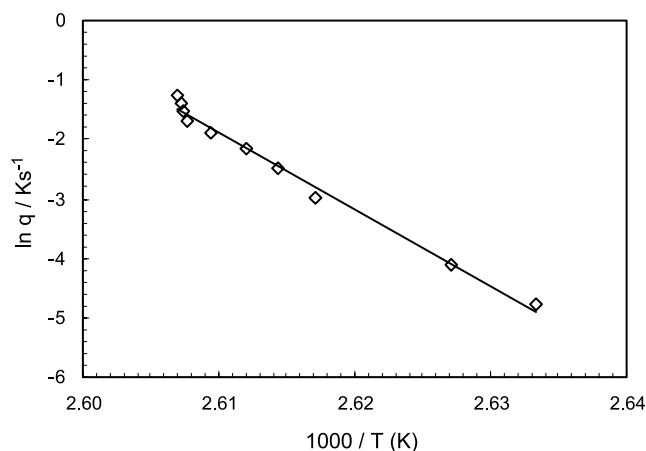


Fig. 8. "Arrhenius plot" (logarithm of the heating rate,  $q$ , as a function of  $1/T_{g,\text{on}}$ ) for the glass transition of raffinose studied by DSC.

amic fragility. Furthermore, the kinetic fragility is related to the large energy barriers between the minima or high activation energy for the structural relaxation. Raffinose thus appears as a very fragile glass former, from both thermodynamic and kinetic points of view, confirming the statement (5) that it is the most fragile glass of those pharmaceutical excipients for which data are available.

### The Mobility in the Crystalline Pentahydrate Form

In the case of the crystalline pentahydrate form, the relaxations observed by TSDC, and shown in Fig. 4A and B, appear in the same temperature regions as those in the amorphous form and also obey to the zero entropy line (see open circles in Fig. 6).

However, important differences between the mobility observed in the two phases are to be underlined, namely, in what concerns the lower temperature relaxation (Figs. 4A and 5A). The first is that the quantity of dipole moment (polarization, defined as the dipole moment by unit of volume) involved in the relaxation is higher in the anhydrous amorphous compared with the crystalline pentahydrate form (see Fig. 3). Another clear difference is that the lower temperature relaxation in the crystal (Fig. 4A) shows a higher structuration. In different words, the motions appear as more individualized, i.e., their diversity seems most sharply defined (see also Fig. 3). This relaxation cannot be considered as a secondary  $\beta$ -relaxation given that this is believed to be a general feature of the amorphous state (23). Taking into account that this mobility in the crystal has low activation energies and negligible activation entropies, the corresponding molecular motions are probably local reorientational motions compatible with the crystal structure.

The features of the relaxation at  $\sim 35^\circ\text{C}$  (Fig. 4B) are similar to those found in the amorphous phase: it is narrow in the temperature axis, it obeys to the zero entropy line, and the representation of  $T_m$  vs.  $T_P$  (open circles in the right-hand side of Fig. 7) does not show the behavior that corresponds to a secondary relaxation. The assignment of this relaxation at the molecular level is difficult, as underlined in the discussion of the amorphous phase mobility.

## CONCLUSIONS

Localized, noncooperative, molecular motions have been identified and characterized in raffinose, in the crystalline pentahydrate form, as well as in the anhydrous amorphous form, below the glass transition temperature.

The relaxations in the crystalline form correspond to individualized motions immersed in a broad and low-intensity relaxation background. In the amorphous state, on the other hand, the relaxations are broader and have a higher dielectric strength. In this amorphous state, a broad secondary  $\beta$ -relaxation was characterized. However, we were not allowed to study the main  $\alpha$ -relaxation by the TSDC technique because of conductivity problems that appear above 100°C. The glass transition of raffinose was characterized by DSC, and the fragility index of this glass former was determined based on the scanning rate dependency of  $T_g$ . It was found that glassy raffinose shows a very high heat capacity jump at the glass transition, and a very high fragility index, indicating that it is an extremely fragile glass former, from both thermodynamic and kinetic viewpoints. Those features suggest that raffinose is a member of a family of carbohydrates with potential abilities as a cryoprotectant of biomacromolecules and organisms.

## ACKNOWLEDGMENT

S. S. Pinto gratefully acknowledges a grant from Fundação para a Ciência e a Tecnologia.

## REFERENCES

1. J. H. Crowe, J. F. Carpenter, and L. M. Crowe. The role of vitrification in anhydrobiosis. *Annu. Rev. Physiol.* **60**:73–103 (1998).
2. J. Buitink and O. Leprince. Glass formation in plant anhydrobiotes: survival in the dry state. *Cryobiology* **48**:215–228 (2004).
3. K. Chatterjee, E. Y. Shalaev, and R. Suryanarayanan. Raffinose crystallization during freeze-drying and its impact on recovery of protein activity. *Pharm. Res.* **22**:303–309 (2005).
4. K. Kajiwara and F. Franks. Crystalline and amorphous phases in the binary system water-raffinose. *J. Chem. Soc., Faraday Trans.* **93**:1779–1783 (1997).
5. K. Kajiwara, F. Franks, P. Echlin, and A. L. Greer. Structural and dynamic properties of crystalline and amorphous phases in raffinose–water mixtures. *Pharm. Res.* **16**:1441–1448 (1999).
6. A. Saleki-Gerhardt, J. G. Stowell, S. R. Byrn, and G. Zograf. Hydration and dehydration of crystalline and amorphous forms of raffinose. *J. Pharm. Sci.* **84**:318–323 (1995).
7. J. J. Moura Ramos, R. Taveira-Marques, and H. P. Diogo. Estimation of the fragility index of indomethacin by DSC using the heating and cooling rate dependency of the glass transition. *J. Pharm. Sci.* **93**:1503–1507 (2004).
8. G. Teyssèdre and C. Lacabanne. Some considerations about the analysis of thermostimulated depolarisation peaks. *J. Phys., D. Appl. Phys.* **28**:1478–1487 (1995).
9. N. T. Correia, C. Alvarez, J. J. Moura Ramos, and M. Descamps. The  $\beta$ - $\alpha$  branching in D-sorbitol as studied by thermally stimulated depolarisation currents (TSDC). *J. Phys. Chem., B* **105**:5663–5669 (2001).
10. N. T. Correia, J. J. Moura Ramos, M. Descamps, and G. Collins. Molecular mobility and fragility in indomethacin: a thermally stimulated depolarisation currents study. *Pharm. Res.* **18**:1767–1774 (2001).
11. J. van Turnhout. *Thermally Stimulated Discharge of Polymer Electrets*, Elsevier Sci. Pub. Co., Amsterdam, 1975.
12. R. Chen and Y. Kirsch. *Analysis of Thermally Stimulated Processes*, Pergamon Press, Oxford, 1981.
13. B. B. Sauer. Thermally stimulated currents: Recent developments in characterization and analysis of polymers. In S. Z. D. Cheng (ed.), *Handbook of Thermal Analysis and Calorimetry*, Vol. 3: Applications to Polymers and Plastics, Elsevier, Amsterdam, 2002, Chap. 15.
14. J. Buitink, I. J. Van den Dries, F. A. Hoekstra, M. Alberda, and M. A. Hemminga. High critical temperature above  $T_g$  may contribute to the stability of biological systems. *Biophys. J.* **79**:1119–1128 (2000).
15. G. A. Jeffrey and D. Huang. The hydrogen bonding in the crystal structure of raffinose pentahydrate. *Carbohydr. Res.* **206**:173–182 (1990).
16. B. B. Sauer, P. Avakian, H. W. Starkweather, and B. S. Hsiao. *Macromolecules* **23**:5119–5126 (1990).
17. K. J. Crowley and G. Zograf. The use of thermal methods for predicting glass-former fragility. *Thermochim. Acta* **380**:79–93 (2001).
18. C. T. Moynihan, A. J. Esteal, J. Wilder, and J. Tucker. Dependence of the glass transition temperature on heating and cooling rates. *J. Phys. Chem.* **76**:2673–2677 (1974).
19. R. Bohmer, K. L. Ngai, C. A. Angell, and D. J. Plazek. Nonexponential relaxations in strong and fragile glass formers. *J. Chem. Phys.* **99**:4201–4209 (1993).
20. R. Bohmer and C. A. Angell. Local and global relaxations in glass-forming materials. In R. Richert and A. Blumen (eds.), *Disorder Effects on Relaxational Processes*, Springer-Verlag, Berlin, Heidelberg, New York, 1994.
21. N. T. Correia, C. Alvarez, J. J. Moura Ramos, and M. Descamps. Molecular motions in molecular glasses as studied by thermally stimulated depolarisation currents (TSDC). *Chem. Phys.* **252**:151–163 (2000).
22. N. T. Correia, C. Alvarez, J. J. Moura Ramos, and M. Descamps. Glass transition relaxation and fragility in the molecular glass forming *m*-toluidine: a study by thermally stimulated depolarisation currents. *J. Chem. Phys.* **113**:3204–3211 (2000).
23. G. P. Johari and M. Goldstein. Viscous liquids and the glass transition. II. Secondary relaxations in glasses of rigid molecules. *J. Chem. Phys.* **53**:2372–2388 (1970).